Molecular Medicine

An Oligodeoxynucleotide with AAAG Repeats Significantly Attenuates Burn-Induced Systemic Inflammatory Responses by Inhibiting Interferon Regulatory Factor 5 Pathway

Yue Xiao,[1] Wenting Lu,[1] Xin Li,[1] Peiyan Zhao,[1] Yun Yao,[1] Xiaohong Wang,[2] Ying Wang,[1] Zhipeng Lin,[1] Yongli Yu,[3] Shucheng Hua,[2] and Liying Wang[1]

[1]Department of Molecular Biology, College of Basic Medical Sciences and Institute of Pediatrics, First Hospital, Norman Bethune Health Science Center, Jilin University, Changchun, China; [2]Department of Respiratory Medicine, The First Hospital of Jilin University, Norman Bethune Health Science Center, Jilin University, Changchun, China; and [3]Department of Immunology, College of Basic Medical Sciences, Norman Bethune Health Science Center, Jilin University, Changchun, China

Previously, we showed that an oligodeoxynucleotide (ODN) with AAAG repeats (AAAG ODN) rescued mice from fatal acute lung injury (ALI) induced by influenza virus and inhibited production of tumor necrosis factor-α (TNF-α) in the injured lungs. However, its underlying mechanisms remain to be elucidated. Upon the bioinformatic analysis revealing that the sequence of AAAG ODN is in consensus with the interferon regulatory factor 5 (IRF5) binding site in the cis-regulatory elements of proinflammatory cytokines, we tried to explore whether AAAG ODN could attenuate burn injury–induced systemic inflammatory responses by inhibiting the IRF5 pathway. Using a mouse model with sterile systemic inflammation induced by burn injury, we found that AAAG ODN prolonged the lifespan of the mice, decreased the expression of IRF5 in the injured skin, reduced the production of TNF-α and IL-6 in the blood and injured skin, and attenuated the ALI. These effects were correlated with AAAG ODN–mediated inhibition of nuclear translocation of IRF5. The data suggest that AAAG ODN could act as a cytoplasmic decoy capable of interfering the function of IRF5 and be developed as a drug candidate for the treatment of inflammatory diseases.
Online address: http://www.molmed.org
doi: 10.2119/molmed.2016.00243

INTRODUCTION

Systemic inflammatory responses can be induced by pathogen infection or non-pathogen tissue damage. Tissue damage, such as burn injury, induces the release of damage-associated molecular patterns such as mitochondrial DNA (mtDNA) and provokes a particularly vigorous whole-body reaction (1). If massively released from damaged tissues, mtDNA, with an abundance of CpG motifs, can activate immune cells through binding of Toll-like receptor (TLR) 9 (1), initiating the TLR9/MyD88 signaling cascade to produce large amounts of proinflammatory cytokines, including tumor necrosis factor-α (TNF-α), interleukin (IL)-6, IL-8 and interferon-α/β (IFN-α/β) (2,3). This signaling cascade can consequently lead to systemic inflammatory response syndrome (SIRS) (2,3). In the TLR9/MyD88 signaling pathway, various transcription factors, such as nuclear factor kappa B (NF-κB) and interferon regulatory factor (IRF) 5, mediate the signaling transduction to activate genes of proinflammatory cytokines (4). IRF5 plays a central role in the inflammatory responses induced by TLR activation. TLR activation induces formation of the MyD88-IRF5-TRAF6 complex (4), which allows relief from the C-terminal self-inhibition of IRF5 by phosphorylation (5). The phosphorylated IRF5 is activated and moves from cytoplasm into nucleoli, where it binds the cis-regulatory element to initiate the transcription of TNF-α/β, IL-6 and IFN-β (6). IRF5 activation is much earlier than IRF3 and 7, which are also transcription factors downstream of the TLR7/9 pathway (7), and specifically upregulate the expression of early inflammatory cytokines such as IL-8 (8) to recruit a large amount of neutrophils to elicit inflammatory responses, resulting in severe tissue

Address correspondence to *Liying Wang or Shucheng Hua, Department of Molecular Biology or Department of Respiratory Medicine, College of Basic Medical Sciences and Institute of Pediatrics, First Hospital, or The First Hospital of Jilin University, Norman Bethune Health Science Center, Jilin University, Changchun, China. Phone: +86 431 81879263. E-mail: wlying@jlu.edu.cn or shuchenghua@eyou.com.*
Submitted December 3, 2016; Accepted for Publication June 6, 2017; Published Online (www.molmed.org) June 14, 2017.

Feinstein Institute for Medical Research
Northwell Health™

damage, such as acute lung injury (ALI) (9). These indicate that IRF5 is involved in the development of systemic inflammatory responses.

There are some experimental clues to support IRF5 as a central regulator in the TLR signaling pathway: (1) When IRF5 is deficient, TLRs (TLR7/9, TLR4, TLR5) are not able to mediate inflammatory responses (4); (2) IRF5-deficient mice resist lethal shock induced by CpG ODN (TLR9 agonist) or lipopolysaccharide (LPS) (TLR4 agonist) (4); (3) individuals with IRF5 dysregulation may develop autoinflammatory diseases (10); (4) in CAL-1 cells, plasmacytoid-like dendritic cell (pDC) line cells, inhibiting IRF5 expression, significantly reduce mRNA expression of IFN-α and IL-6 (7); and (5) IRF5–/– mice have a significantly reduced number of neutrophils recruited into the lung post LPS challenge and reduced acute lung injury (11). These studies demonstrate that blockade of IRF5 might be an effective method for downregulating production of inflammatory cytokines and therefore ameliorating acute inflammation. In our previous work, an oligodeoxynucleotide with AAAG repeats (AAAG ODN) was demonstrated to rescue mice from influenza virus–induced ALI and inhibit the activation of TNF-α in the mouse lung tissue (12). Since the sequence of AAAG ODN is in consensus with the DNA-binding site of IRF5, we deduced that AAAG ODN could interfere with the function of IRF5 and be used to inhibit systemic inflammatory responses. Various reagents have been found to alleviate severe inflammatory reactions by interfering with IRF5. Mangiferin downregulates IRF5 expression, and therefore inhibits the activation of macrophages and the release of proinflammatory cytokines (13). Baicalin alleviates dextran sodium sulfate–induced colitis by decreasing LPS-induced IRF5 expression (14). Nanoparticle-delivered IRF5 siRNA promotes efficient transition of macrophages from M1 to M2 and functional recovery after spinal cord injury in mice (15).

In this study, we established a mouse model with systemic inflammatory response syndrome (SIRS) induced by burn injury to find the possible mechanisms of how AAAG ODN inhibits systemic inflammatory responses. We found that AAAG ODN could alleviate the severe inflammatory responses by interfering with the function of IRF5.

MATERIALS AND METHODS

Animals

Six- to eight-week-old BALB/c female mice were purchased from the Experimental Animal Center, Medical College of Norman Bethune, Jilin University, and maintained in microisolator cages under specific pathogen-free conditions. The experimental manipulation of mice was undertaken in accordance with the National Institute of Health Guide for the Care and Use of Laboratory Animals, and with the approval of the Scientific Investigation Board of Science and Technology of Jilin Province, China. All mice received humane care in compliance with the 2011 Guide for the Care and Use of Laboratory Animals published by the National Institutes of Health (16).

Cell Culture

THP-1 cells, human monocytic cell line cells derived from an acute monocytic leukemia patient, and HEK293 cells, IRF5 overexpressing cells, were maintained in RPMI 1640 medium supplemented with 10% (V/V) fetal bovine serum (FBS) (Gibco) and antibiotics (100 IU penicillin/ml and 100 IU streptomycin/ml). All cells were cultured at 37°C in a 5% CO_2 humidified incubator.

To detect the nuclear translocation of IRF5, THP-1 cells were plated into 6-well plates at a density of 2×10^6 cells/well, cultured with RPMI 1640 medium containing 2% FBS, CpG 2006 (2 μg/ml), AAAG ODN (8 μg/ml) or control ODN (8 μg/ml). At 24 h post-incubation, the cells were harvested and lysed to separate cytoplasmic and nuclear fractions. The nuclear translocation of IRF5 was detected by Western blotting.

Oligodeoxynucleotides and Antibodies

All oligodeoxynucleotides (ODNs) were synthesized by Takara Biotechnology Company (Dalian, China). The following ODNs were used in this study: AAAG ODN (5′-AAAGAAAG AAAGAAAGAAAGAAAG-3′), control ODN (5′-CCTCCTCCTCCTCCTCC TCCTCCT-3′) and CpG 2006 (5′-TCGT CGTTTTGTCGTTTTGTCGTT-3′). The ODNs with full-phosphorothioate modification were diluted in sterile PBS buffer and had no detectable endotoxin (Limulus Amebocyte Lysate assay, Associates of Cape Cod, East Falmouth, MA, USA).

The following antibodies were used for Western blotting: RelA/NF-κB p65 (MAB5078, R&D Systems, Minneapolis, MN, USA), MyD88 (AF3109, R&D Systems), glyceraldehyde-3-phosphate dehydrogenase (60004-1-Ig, Proteintech, Rosemont, IL, USA), IRF5 (ab33478, Abcam, Cambridge, MA, USA), TLR9 (ab6257, Abcam), proliferating cell nuclear antigen (13110S, Cell Signaling Technology, Danvers, MA, USA), β-actin (3700S, Cell Signaling Technology), rabbit anti-goat IgG (bs-0294R, Bioss Antibodies, Woburn, MA, USA), goat anti-mouse IgG (120344, Jackson Laboratory, Bar Harbor, ME, USA), and goat anti-rabbit IgG (116154, Jackson Laboratory). The monoclonal antibodies of APC rat anti-mouse Ly6G (560599), APC rat anti-mouse IL-6 (561367) and PE-Cy7 rat anti-mouse TNF-α (557644) were purchased from BD Biosciences (San Jose, CA, USA).

Burn Injury Model

Before establishing the burn injury model, BALB/c female mice were fasted for 10–12 h and allowed to drink normally. The mice were anesthetized intraperitoneally with 10% chloral hydrate (~140 μl/20 g v/w) (Major Pharmaceuticals, Livonia, MI, USA). The dorsal hair was clipped with an electronic shaver and the residual hair was further removed with hair removal cream. The exposed skin was cleaned

gently with sterile gauze containing water and sterilized with iodine tincture. The iodine tincture from the prep area was wiped off using gauze containing 70% isopropyl alcohol. A single full-thickness burn (~30% total body) was introduced with electrocautery (400–430°C for 3 s) on the mid-dorsum of each mouse. This protocol was performed as previously described (17). The anesthetic injury was nonlethal (<1% mortality). Animals were resuscitated with warm water bags (40–45°C). Then they were placed alone in separate cages and maintained under standard conditions in the animal facility (as described above). The experimental procedures were approved by the Ethics Committee of College of Basic Medical Sciences, Jilin University.

Mice were treated with ODNs intraperitoneally or topically. For intraperitoneal application, 0.1 ml of 25 μg ODNs or PBS was injected into the burn-injured mice twice at a 24 h interval, starting immediately after injury. The ODN dose was determined in previous studies (12). For topical application, 40 μl of 25 μg ODNs or PBS was applied to the wound twice, at a 24 h interval, starting immediately after injury. Sham animal treatment consisted of anesthesia and resuscitation with water bags. Peripheral white blood cells (WBCs) of the burn-injured mice were obtained from blood sampled via mouse eyeball. To collect skin tissues, animals were euthanized, and skin tissues were stored at –80°C until further processing.

Quantitative Real-Time Polymerase Chain Reaction

The blood samples were collected in tubes containing 3.8% sodium citrate (1/9 v/v) and centrifuged (2000 g for 5 min at 4°C). The red blood cells were lysed using ACK buffer (1/9 v/v) (NH4Cl 8024 mg/L, KHCO3 1001 mg/L, Na2EDTA 3.7 mg/L, pH 7.2–7.4) for 7–10 min, followed by washing and centrifugation steps repeated twice. The obtained WBCs and 100 mg of skin tissue as described above were homogenized in 1 ml Trizol reagent (CWBIO, CW0580S) and reverse transcribed using cDNA Synthesis Kit (TransGen Biotech, Beijing, China), respectively. Quantitative real-time polymerase chain reaction (RT-PCR) was performed using two-step SYBR green qPCR assays, and the target mRNA was identified by the specific primers as follows (forward and reverse primers, respectively): TLR9: 5′-ACCCTGGAAGAGCTAAACCTG-3′ and 5′-CAGTTGCCGTCCATGAATAGG-3′; MyD88: 5′-TCGCAGTTTGTTTGCC TG-3′ and 5′-TGTAAAGGCTTCTCGGA CTCC-3′; NF-κB: 5′-GCATTCTG ACCTTGCCTAT-3′ and 5′-CCAGTCT CCGAGTGAAGC-3′; IRF5: 5′-AGCG GGAAGTCAAGACGAAGCTCT-3′ and 5′-CTGAGAACATCTCCAGCAGCA-3′; β-actin:5′-GATCAAGATCATTGCTCCTC CTG-3′ and 5′-AGGGTGTAAAACG-CAGCTCA-3′; TNF-α: 5′-GGCTCCAG GCGGTGC TTGTT-3′ and 5′-GGCTTG TCACTCGGGGTTCG-3′; IL-6: 5′-GG ATACCACTCCCAA CAGACC-3′ and 5′-TCCAGTTTGGTAGCATCATCA-3′. The procedure of the target mRNA amplification was as follows: 1 cycle at 95°C (30 s) followed by 40 cycles at 95°C (5 s) and 64°C (31 s). Each assay plate included negative controls with no template. The relative amount of gene expression was analyzed with the $2^{-\Delta\Delta Ct}$ method using the Step One™ real-time PCR system (Applied Biosystems).

The mtDNA level was measured by absolute quantification RT-PCR, as previously described (18). The DNA was isolated from plasma using the DNeasy Blood and Tissue Kit (Qiagen, Hilden, Germany), according to the manufacturer's instructions. The primer sequences were designed as 5′-AC TGTTCGCAGTCATAGCCA-3′ and 5′-AGCGAAGAATCGGGTCAAGGT-3′. The thermal profile for detecting mtDNA was carried out as follows: 1 cycle at 95°C (30 s) followed by 40 cycles at 95°C (5 s), 52°C (10 s) and 72°C (10 s). Standards for mtDNA were prepared from mitochondria isolated from liver cells of the mice.

Western Blotting

The samples for Western blotting analysis were prepared from skin tissues or cultured cells. The skin tissues were lysed in ice-cold RIPA buffer (150 mM NaCl, 50 mM Tris, pH 7.4, 1% NP-40, 0.5% sodium deoxycholate, 0.1% SDS and PMSF). The lysates were centrifuged (14,500 g for 10 min at 4°C) and the supernatant was collected, quantified using a BCA protein assay kit (Wanleibio, Shenyang, China). The cultured THP-1 cells were collected and lysed to separate cytoplasmic and nuclear fractions using the ProteinExt® Mammalian Nuclear and Cytoplasmic Protein Extraction Kit (TransGen Biotech). The lysates from the tissues or cells were separated by 12% SDS-PAGE. Gels were blotted using PVDF membranes (Millipore, Billerica, MA, USA). The membranes were blocked for 2 h at room temperature (22–25°C) with Tris-buffered saline containing 5% dried nonfat milk and probed with various antibodies overnight at 4°C. After being washed with TBST (150 mM NaCl, 10 mM Tris-HCl [pH 8.0], 0.5% Tween 20) three times at 10 min intervals, the membranes were incubated with horseradish peroxidase–labeled secondary antibodies for 1 h at room temperature. After being further washed, the membranes were treated with West Femto Substrate Trial Kit (Thermo Scientific) and the interesting protein bands were visualized by Amersham Biosciences Hyperfilm ECL (GE Healthcare Life Sciences).

Pull-Down Assay

Oligodeoxynucleotides, AAAG ODN and control ODN were biotin-labeled at the 5′- end, and 1 μg of labeled ODNs was incubated with magnetic streptavidin beads (50 μl) for 1 h at room temperature. Beads were washed and incubated with lysates (300 μg) of HEK293 cells transfected with IRF5 plasmid overnight at 4°C and then extensively washed. The specifically bound IRF5 was detected by Western blot as described above.

Histological Analysis and Immunohistochemistry

The skin and lung tissues of the burn-injured mice were fixed in 4% (w/v) paraformaldehyde, embedded into paraffin, sectioned, stained with hematoxylin and eosin, and observed under the microscope. Four parameters – hyaline membranes, interstitial infiltrates, congestion and hemorrhage – were taken into account in the microscopic observation of the tissues. Pathological scores of the lung tissues were determined based on the scale: 0, no pneumonia; 1, mild interstitial pneumonia (<25% of the lung); 2, moderate interstitial pneumonia (25–50% of the lung); 3, severe interstitial pneumonia (>50% of the lung). For immunohistochemistry (IHC), the tissue sections were dewaxed, rehydrated and then incubated in citrate buffer at 95°C for 15 min, enabling antigen retrieval. After being treated with hydrogen peroxide for 10 min at room temperature, the sections were incubated with 1:50 diluted mouse anti-IRF5 monoclonal antibodies at room temperature for 2 h and then washed, followed by incubation with horseradish peroxidase–streptavidin complex (Maixin, Fuzhou, China) for 30 min at 37°C. The sections were then stained with DAB (Maixin) and counterstained with hematoxylin. All steps were performed at room temperature unless otherwise specified. $IRF5^+$ cells were scored as 1, 2, 3, 4, 5 or 6 when the percentage of $IRF5^+$ cells in the total 500 cells in each sample was <3%, 3–6%, 6–9%, 9–12%, 12–15% or 15–18%, respectively.

Flow Cytometry

For surface staining, the WBCs were stained with APC rat anti-mouse Ly6G for 30 min at 4°C in the dark, followed by washing twice with PBS. For intracellular staining, the whole blood was harvested at 2 h post burn and diluted 1:1 with RMIP1640 medium. The cells were added into a 12-well plate and incubated with monensin (eBioscience) for 2 h in 5% CO_2 at 37°C. Then, the cells were collected and fixed with 4% paraformaldehyde and permeabilized with 0.1% saponin, followed by staining with APC rat anti-mouse IL-6, PE-Cy7 rat anti-mouse TNF-α and V450 rat anti-mouse Ly6G. All stained cells were analyzed by Accuri C6 (BD) and FACSCanto (BD) flow cytometers. Live cells were carefully gated by forward and side scattering. Data were analyzed with FlowJo software (v. 7.6.1).

Lung Wet/Dry Ratio

The ratio of wet to dry weight was used as an indicator of pulmonary edema. Half of the left lung samples were separated and weighed. Then the lobe was dried at 60°C for 48 h to obtain the dry weight.

Statistical Analysis

Comparisons between groups were conducted using analysis of unpaired *t* tests. *P* value < 0.05 (95% confidence interval) was considered to be statistically significant. Statistics were analyzed using GraphPad Prism 5.0 for Windows.

All supplementary materials are available online at www.molmed.org.

RESULTS

Establishment of a Mouse Model with Sterile Systemic Inflammatory Responses Induced by Skin Burn Injury

To establish a mouse model with sterile systemic inflammatory responses, we burned the skin of BALB/c female mice using electrocautery, observed histopathological changes of skin and lung, detected neutrophils and mtDNA in blood, and recorded the survival of the mice. In the sections of burn-injured skin collected at 24 h post burn, we found that the injured dermis appeared to have a disordered arrangement of collagen fibers, cavity formation and cell necrosis, while the muscle underneath the dermis was integrated, though the neutrophils were increasingly infiltrated in the muscular fascia (Figure 1A). Above all, the burn injury was considered to be a third-degree burn. As to survival, around 24 h post burn injury, the mice began to die. After being burned, 50% of the mice were dead in 36 h and 100% of the mice were dead in 42 h (Figure 1A). We checked the internal organs of the injured mice and found that there were bleeding points, hyperemia and infiltration of neutrophils in lung tissues at 24 h post burn injury (Figure 1B). When counting neutrophils in peripheral blood of the mice at 2 h and 24 h post burn injury, we found the percentage of $Ly6G^+$ cells in WBCs was significantly increased ($P < 0.05$). Unexpectedly, we found the expression level of Ly6G on neutrophils from burn-injured mice was significantly decreased ($P < 0.05$) (Figure 1C). In addition, we also found that mtDNA levels in plasma of the burn injured mice were obviously elevated ($P = 0.0263$) (Figure 1D). These results suggest that burn injury of the skin can result in sterile systemic inflammatory responses, and mtDNA released as a damage-associated molecular pattern may trigger the response.

Influence of AAAG ODN on the Survival of Burn-Injured Mice

To test whether AAAG ODN could rescue burn-injured mice from death, we intraperitoneally injected the mice with AAAG ODN at 25 μg per mouse twice at a 24 h interval, starting immediately after burn injury. The survival of the mice was recorded. The results show that AAAG ODN significantly prolonged survival of the burn-injured mice ($P < 0.05$). At 36 h post burn injury, five of the eight mice in the AAAG ODN group were alive, while all of the mice in the PBS group were dead and only two of the mice injected with control ODN survived (Figure 2A). Surprisingly, when applied through the burn-injured skin at the same dosage and interval as for intraperitoneal injection, AAAG ODN failed to rescue the mice (Figure 2B). The results indicate that the burn-injured mice succumbed to systemic inflammatory response and AAAG ODN could rescue the mice by inhibiting the response.

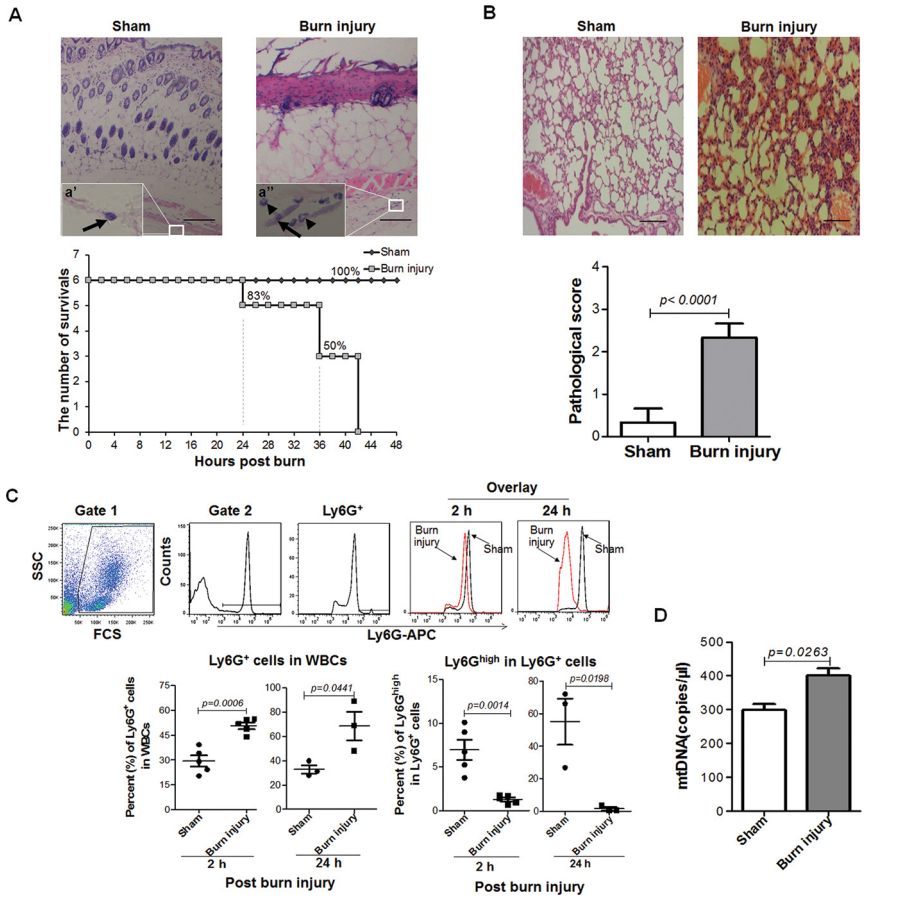

Figure 1. Sterile systemic inflammatory responses induced by skin burn injury in mice. Female BALB/c mice (n = 6 mice/group) were burned with electrocautery at 400–430°C for 3 s and their survival was recorded. The skin and lung tissues of burn-injured mice and normal mice were collected at 24 h post burn for histological analysis. (A) Skin pathological changes (hematoxylin and eosin (H&E) staining, magnification x 40) and survival curves of mice. (a') and (a'') Higher magnification (x 400) of fibroblasts, denoted by arrows, and neutrophils, denoted by arrowheads, in muscular fascia. Scale bars = 200 μm. (B) Lung pathological changes (H&E staining, magnification x 40) and scores. Scale bars = 200 μm. (C) Ratios of $Ly6G^+$ cells in WBCs and $Ly6G^{high}$ in $Ly6G^+$ cells. $Ly6G^+$ cells represent the neutrophils. Data are represented as mean ± standard error of the mean (SEM) (n = 3–5 mice/group). (D) The mtDNA copies in plasma of sham or burn-injured mice were detected by qPCR. Data are represented as mean ± SEM (n = 3 mice/group).

Effect of AAAG ODN on the Expression of Inflammation Related Factors in Burn-Injured Skin in Mice

To study whether the effect of AAAG ODN on reducing burn injury–induced death in mice was caused by inhibiting the initiation of inflammation, we detected the levels of inflammation-related factors in the burn-injured skin of mice treated with either AAAG ODN or control ODN. The results show that burn injury significantly stimulated the transcription of TLR9 ($P < 0.05$), MyD88 ($P < 0.01$), NF-κB ($P < 0.05$) and IRF5 ($P < 0.01$) mRNA in the injured skin at 0.5 h post burn (Figure 3A). AAAG ODN could significantly downregulate the transcription of IRF5 mRNA ($P < 0.01$) but not TLR9, MyD88 or NF-κB mRNA, and control ODN did not affect the transcription of any of the factors (Figure 3A). To confirm the results, we detected the protein levels of TLR9, MyD88, NF-kB and IRF5 in the injured skin tissue by Western blotting. We found that burn-injury stimulation induced obvious elevation the protein levels of TLR9, MyD88, NF-κB and IRF5 in the burn-injured skin ($P < 0.05$) (Figure 3B), AAAG ODN only reduced the expression level of IRF5 ($P < 0.05$), and control ODN had no effect on the expression of TLR9, MyD88, NF-κB and IRF5 (Figure 3B). To find the types of cell whose IRF5 expression was interfered by AAAG ODN, we stained the injured skin tissues by immunohistochemistry using anti-IRF5 mAb, and found that AAAG ODN reduced IRF5 expression in the keratinocytes and fibroblasts of the burned skin (Figure 3C). These results suggest that AAAG ODN could inhibit inflammation initiation by interfering with the function of IRF5 in skin tissues.

Inhibitory Effect of AAAG ODN on Production of Inflammatory Cytokines in Burn-Injured Mice

After finding that AAAG ODN was capable of downregulating IRF5 expression, we tested whether it could inhibit the expression of IRF5 downstream inflammatory cytokines, including TNF-α and IL-6. First, we detected TNF-α and IL-6 mRNA levels of the burn-injured skin at three time points post burn injury. The results reveal that mRNA levels of TNF-α and IL-6 were obviously elevated at the injured skin in mice early and 24 h post burn injury ($P < 0.05$). AAAG ODN displayed an inhibitory role in mRNA transcription of TNF-α in the burn-injured skin at 0.5 h and 24 h post burn injury, and also on the mRNA transcription of IL-6 in the burn-injured skin at 0.5 h and 4 h post burn injury (Figure 4A). To observe whether the burn injury could induce systemic production of inflammatory cytokines and AAAG ODN could inhibit the production response, we detected mRNA versus protein expression of TNF-α and IL-6 in circulating WBCs. We found that the burn injury significantly promoted the expression of TNF-α

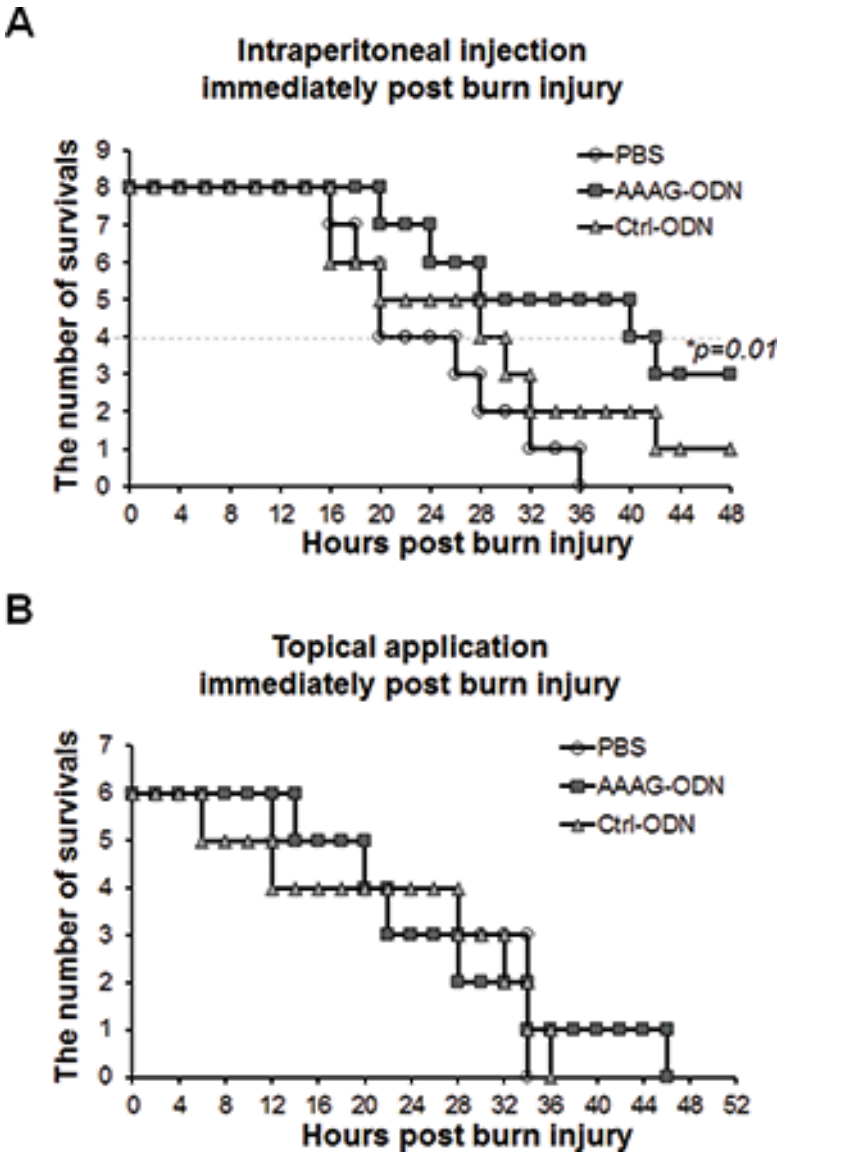

Figure 2. Effect of AAAG ODN on the survival of burn-injured mice. Burn-injured mice were treated with AAAG ODN or control ODN or PBS by (A) intraperitoneal or (B) topical application and their survival was recorded.

mRNA at 0.5 h, 4 h and 24 h, and IL-6 mRNA at 0.5 h post burn injury. The increased mRNA levels of TNF-α and IL-6 could be significantly reduced by AAAG ODN but not by control ODN (Figure 4B). Also, the burn injury obviously induced protein expression of TNF-α and IL-6 in the WBCs of the injured mice and AAAG ODN, not control ODN, significantly downregulated the expression (Figure 4C). To identify the TNF-α/IL-6 producing cells, we stained the WBCs with mAbs against Ly6G, IL-6 and TNF-α, and found that the percentage of $Ly6G^+TNF\text{-}\alpha^+$ cells and $Ly6G^+IL\text{-}6^+$ cells was increased by an average of five-fold and three-fold in the WBCs of burned mice, respectively, and that the numbers of $Ly6G^+TNF\text{-}\alpha^+$ cells and $Ly6G^+IL\text{-}6^+$ cells in the burned mice treated with AAAG ODN were similar to those in the sham mice (Figure 4D). All of the above results suggest that AAAG ODN could lessen the burn injury–induced systemic inflammatory response by reducing the production of TNF-α and IL-6 in the circulating neutrophils.

Effect of AAAG ODN on Reducing Pulmonary Inflammation in Burn-Injured Mice

Owing to a high risk of multiple organ failure seen in burn-induced ALI (19,20), we tested whether the AAAG ODN could reduce the lung injury of the model mice. Histopathologically, at 24 h post burn injury, the lungs of burn-injured mice treated with PBS and control ODN displayed thickened and congested alveolar walls and numerous infiltrated inflammatory cells. In contrast, the mice treated with AAAG ODN showed no or few changes in their lung tissues (Figure 5A). The pathological score of the lung tissues in the burn-injured mice treated with AAAG ODN was lower than that in the mice treated with PBS and control ODN (Figure 5B). To assess whether edema occurred in the lungs of burn-injured mice, we measured the wet and dry weight of lung tissues and found no difference in wet/dry ratios of the lungs isolated at 24 h post burn injury (Figure 5C). The results suggest that AAAG ODN could reduce ALI in mice injured by burn.

The Interfering Role of AAAG ODN on IRF5

Since AAAG ODN can enter cells to modulate IRF5 expression, it is reasonable to presume that it may also interact with IRF5. To determine the relationship of AAAG ODN and IRF5, we performed a pull-down assay using IRF5-transfected HEK293 cell lysate to interact with AAAG ODN, followed by Western blotting with anti-IRF5 antibody. The results show that the cell lysate contained abundant IRF5 protein and AAAG ODN could partially pull down IRF5. Surprisingly, control ODN could pull down IRF5 proteins (Figure 6A). To further explore whether the AAAG ODN could inhibit IRF5 nuclear translocation, we cultured the THP-1 cells with AAAG ODN, control ODN or PBS in the presence of

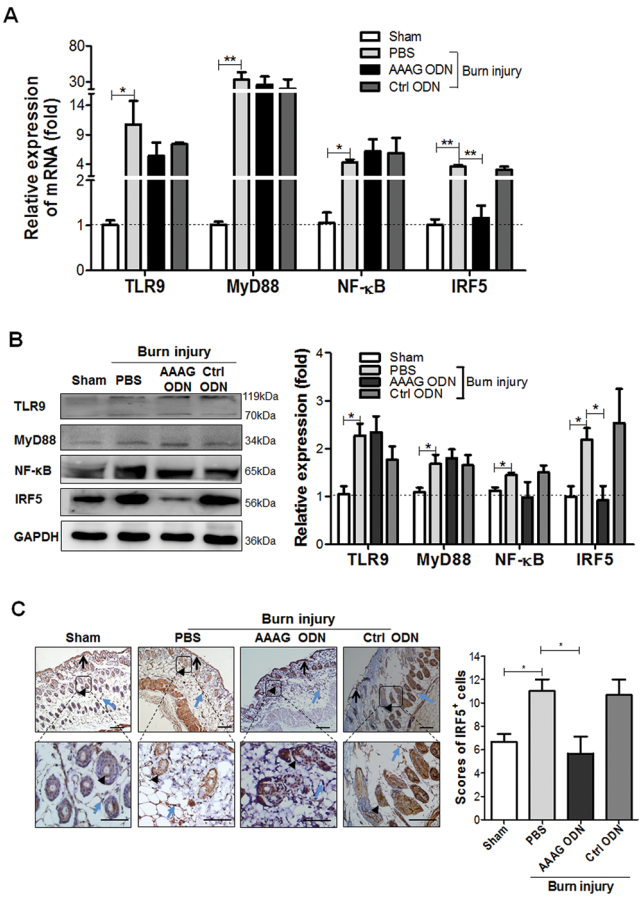

Figure 3. Effect of AAAG ODN on the TLR9-IRF5 pathway in burn-injured skin of the mice. The skin tissues collected from sham and burn-injured mice (3/group) at 0.5 h post burn injury were detected for (A) mRNA and (B) protein levels of TLR9, MyD88, NF-κB and IRF5 by qPCR and Western blot, and for (C) IRF5 expression by immunohistochemistry (IHC). Arrows, black arrowheads and blue arrowheads denote keratinocytes in the epidermis, keratinocytes in hair follicles and fibroblasts in dermis, respectively. Brown represents expression of IRF5 protein. The bars in column charts represent SEM for means; *$P < 0.05$, **$P < 0.01$, ***$P < 0.001$. In the IHC images, scale bars correspond to 100 μm and magnification is x 200 (upper panel) and x 400 (lower panel).

CpG 2006 for 24 h. This time point was chosen by kinetic observation, shown in Supplementary Figure S3. The cells were collected and separated into cytoplasmic and nuclear fractions for detecting IRF5. It was found that AAAG ODN, not control ODN, obviously reduced the IRF5 in nuclear fractions (Figure 6B), indicating that IRF5 nuclear translocation could be inhibited by AAAG ODN.

DISCUSSION

BALB/c and C57BL/6 mice were commonly chosen as model animals to investigate thermal injury–induced immune dysfunction to find approaches to reverse the dysfunction (21). In this study, by using BALB/c mice, we demonstrated that AAAG ODN could suppress systemic inflammation caused by severe burn injury, and therefore prolong the survival of the mice. Evidently, BALB/c mice were used by other groups to observe the effect of low-energy shock waves on attenuating acute pro-inflammatory cytokine expression (22) and the effect of endogenous hydrogen sulfide on aggravating burn-associated systemic inflammation (23), and to evaluate whether a nonspecific phosphodiesterase inhibitor could attenuate burn-induced inflammatory signaling via the mitogen-activated protein kinase pathway (24). Recently, C57BL/6 mice have also been adopted to investigate inflammatory gene expression induced by burn injury (25). Comparatively, BALB/c and C57BL/6 mice could exhibit similar inflammatory responses to burn injury, manifested by the production of TNF-α and IL-10 from splenic macrophages stimulated with LPS (21). Informatively, the data obtained from both BALB/c and C57BL/6 mice could provide insights for clinical settings, because the expression profiles of TNF-α and IL10 change significantly in burn patients compared with healthy persons (26,27). Moreover, the similarities of the changes in gene expression and a number of similar pathways/biogroups between the mouse burn models and human burn conditions also suggest that the mouse model could be used to mimic human responses to inflammation (28,29).

In this study, a 30% total body surface area burn injury induced 100% mortality in BALB/c mice. The mortality rate is obviously higher than the 50% reported by other groups (30). The discrepancy might not be due to the depth of the burn injury, because pathological examination showed that the muscle underneath the burned dermis was still integrated, indicating a third-degree burn of the skin (Figure 1A). In addition, the gender of the mice and the treatment of pre-burn starvation may also have contributed to the high mortality. Female mice were used in this study, and they were reported to be more vulnerable to sustained burn injury compared with males (31). Depriving food was found to markedly increase the sensitivity of mice to LPS toxicity, manifested by LPS (15 mg/kg) causing 20% lethality in fed mice, while 100% of fasted mice succumbed (32). Starvation also enhances the severity of inflammatory disease in humans. Prolonged starvation could

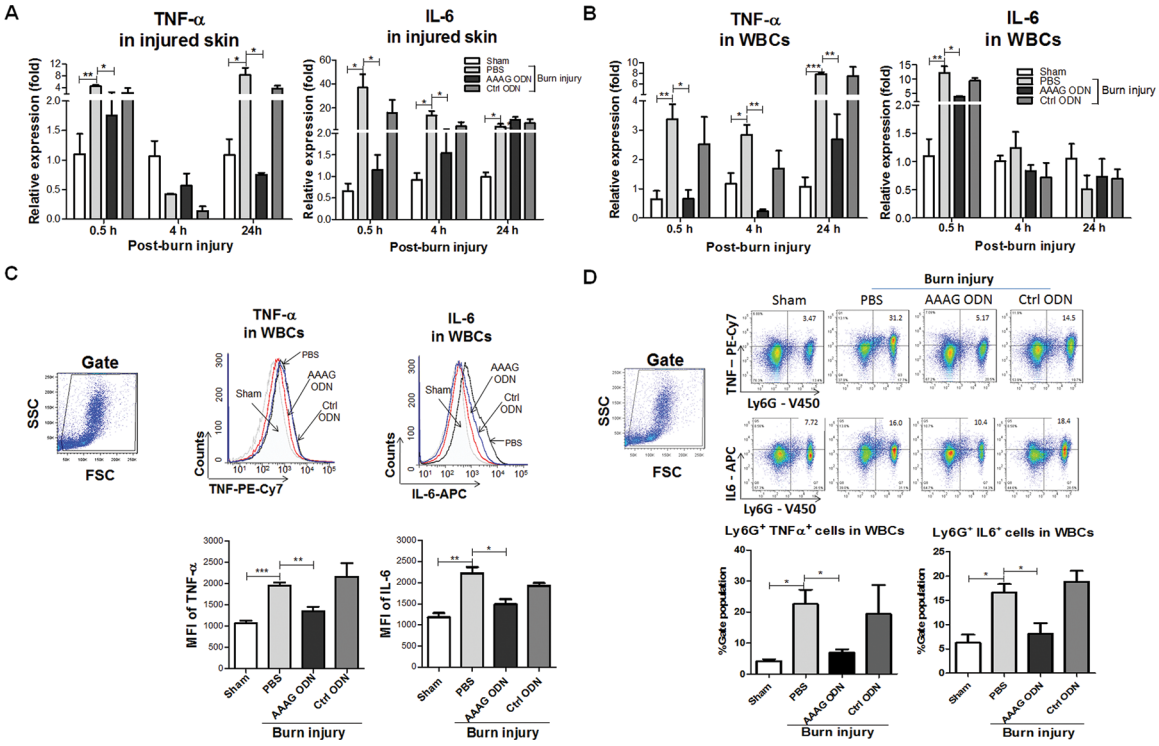

Figure 4. Effect of AAAG ODN on TNF-α and IL-6 production in skin tissues and WBCs of burn-injured mice. (A) Burn-injured skin tissues and (B) peripheral white blood cells (WBCs) collected at different time points post burn were used to detect the mRNA expression of TNF-α and IL-6 by qPCR. The WBCs harvested at 2 h post burn were treated with monensin in vitro for 2 h, and then subjected to flow cytometric analysis to detect (C) intracellular expression of TNF-α and IL-6 and (D) the percentage of TNF-α or IL-6 positive neutrophils. Data are represented as mean ± SEM (n = 3 mice/group). *$P < 0.05$, **$P < 0.01$, ***$P < 0.001$.

lead to the development of inflammatory changes like SIRS in patients with intestinal endotoxin–induced inflammation (33). In addition, massively produced TNF-α and IL-6 in the development of SIRS contributed to the high mortality in patients with severe burn injury (34). As shown in Figure 4, 30 min post burn, TNF-α and IL-6 were readily detected in circulating WBCs, as well as burned skin. As reported, the rapidness was accompanied by burn injury–induced activation of NF-kB within 30 min and significantly increased IL-6 production in lung tissue (35). Noticeably, globally inflammatory reactions were rapidly initiated by burn injury. As shown in Supplementary Figure S1, within 30 min post burn, neutrophils were massively mobilized into the blood. The neutrophils were activated by mtDNA to secrete huge amounts of TNF-α and IL-6 (1), causing rapid systemic inflammation. In addition to the neutrophils, local keratinocytes and fibroblasts in the burned skin could also contribute to the rapid systemic inflammation by producing inflammatory cytokines. The keratinocytes and fibroblasts were identified as TLR9 and IRF5 expressing cells (36–38), and therefore could be activated by the mtDNA released from burned skin through the TLR9-MyD88-NF-κB/IRF5 pathways. As shown in Figure 3, IRF5 expression was accompanied by increased expression of TLR9, MyD88 and NF-κB in the burned skin. The increased expression of IRF5, TLR9, MyD88 and NF-κB could be correlated with activation of the TLR9-MyD88-NF-κB/IRF5 pathways. The correlation could be supported by data showing that the upregulation of TLR9, MyD88 and NF-κB, induced by mtDNA (23) or other CpG rich DNA (39), led to the activation of TLR9-MyD88-NF-κB/IRF5 signaling. Moreover, as reported, IRF5 expression could be autoregulated via a positive feedback loop, in which IFN-α expression is upregulated by IRF5 and in turn IFN-α increases IRF5 expression (40).

Structurally, AAAG ODN was in consensus with the IRF5 binding site in the cis-regulatory elements of proinflammatory cytokines such as TNF-α and IL-6 (2,41). Thus, AAAG ODN could bind and interfere with IRF5, resulting in reduced production of the proinflammatory cytokines TNF-α and IL-6. This interference was demonstrated in this study. As shown in Figure 6, nuclear translocation of IRF5 was induced by CpG 2006 and inhibited by AAAG ODN in cultured cells. This inhibition could be attributed to the interaction between IRF5 and AAAG ODN, since IRF5 in cultured cells could be pulled down by AAAG ODN. Unexpectedly, the control ODN consisting of CCT repeats also

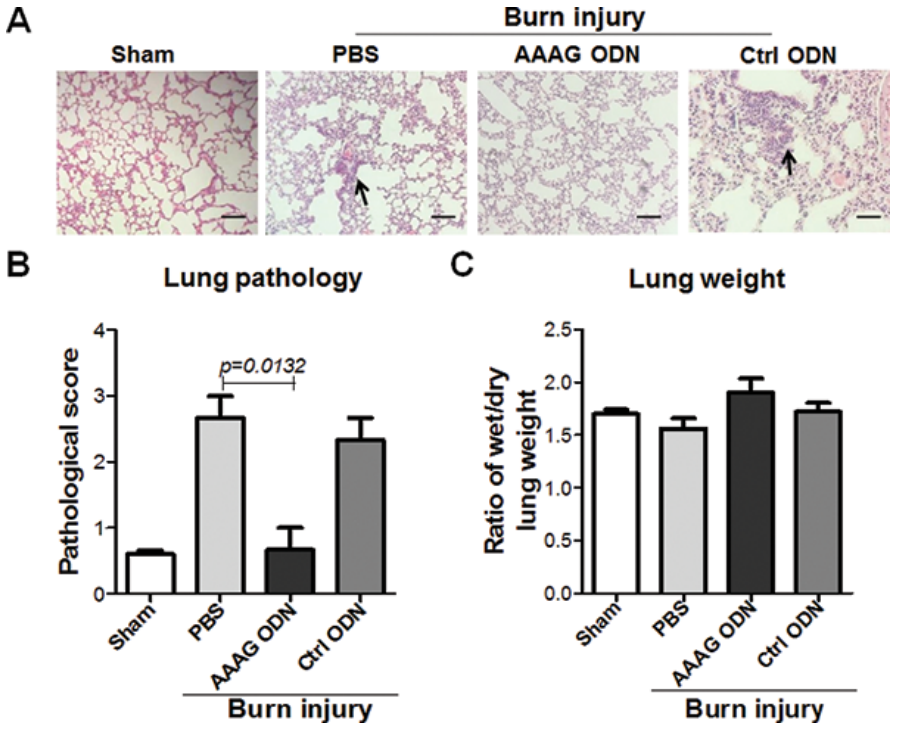

Figure 5. Alleviating role of AAAG ODN on ALI of burn-injured mice. The lungs of the mice at 24 h post burn were weighed and sectioned for H&E staining. The slices were (A) observed for pathological changes and (B) evaluated for pathological scores. (C) The wet/dry weight ratio of lung was used as a parameter to denote acute pulmonary edema. The black arrows indicate the infiltrated inflammatory cells. Data are represented as mean ± SEM (n = 3 mice/group). *$P < 0.05$, **$P < 0.01$, ***$P < 0.001$. Scale bars = 50 μm, magnification x 200.

pulled down IRF5 from the cells. To understand this, we compared IRF5 binding DNA sequence with the sequence of the control ODN using an online analysis tool (http://jaspar.binf.ku.dk/ and http://www.genomatix.de/), and failed to find the correlation. Unlike AAAG ODN, the control ODN couldn't inhibit nuclear translocation of IRF5 and was unable to downregulate the production of TNF-α and IL-6. Thus, we might presume that although the control ODN could bind IRF5, it was insufficient to interfere with IRF5 to activate pro-inflammatory cytokine genes as AAAG ODN did. Interestingly, our data show that AAAG ODN not only bound IRF5, but also downregulated the expression of IRF5. The downregulation might be attributed to ubiquitination of IRF5. As reported, IRF5 bound to an apoAI mimic was ubiquitinated, and then degraded (42).

Noticeably, AAAG ODN, when topically applied, failed to rescue the mice with severe burn injury from death. We tried to treat the mice immediately after burning with AAAG ODN at a reduced dosage (6.25 μg/mouse) four times at 3 h intervals, and failed to prolong survival of the burned mice (Supplementary Figure S2A). Alternatively, we started to treat the mice at 2 h post burn by using AAAG ODN at the dosage, frequency and intervals as described above, and found that three of the five burned mice that received AAAG ODN were still alive at 60 h post burn, while the mice treated with PBS were all dead (Supplementary Figure S2B). This observation suggests that the efficacy of the topically applied AAAG ODN could be improved if the dose and dosing schedules were appropriately adjusted. In addition, an appropriate dosage form may be required to ensure adequate localization or penetration of the topically applied AAAG ODN (43,44). In contrast, intraperitoneal application of AAAG ODN rescued the burned mice from death, suggesting that intraperitoneally applied AAAG ODN could readily reach the injured skin and blood circulation. As shown in Figure 4, intraperitoneally applied AAAG ODN significantly reduced the levels of TNF-α and IL-6 and the $Ly6G^+TNF\text{-}\alpha^+$ cells and $Ly6G^+IL\text{-}6^+$ cells in blood, and therefore rescued the burned mice.

Based on the accumulated evidence, ALI, as one of main complications post burn injury, was associated with burn-induced high mortality (19). Consistently, ALI was observed in severe burn-injured mice and caused the death of the mice. ALI has been attributed with burn-induced systemic production of a large amount of TNF-α (45). In rodents, a burn-induced elevation of TNF-α in serum was correlated with ALI (20,46). In humans, elevated serum levels of TNF-α was considered to have predictive value for development of ALI/adult respiratory distress syndrome and associated with patient mortality (47). Thus, reducing the systemic production of TNF-α could be an approach to save severe burned mice by reducing the occurrence of ALI. In this study, we demonstrated that the lifesaving intraperitoneal injection of AAAG ODN downregulated TNF-α in the WBCs of burn-injured mice, and this downregulation was associated with reduced ALI, manifested by reduced inflammatory cell infiltration in the lungs. Similar results were also observed in our previous work showing that AAAG ODN treatment significantly reduced neutrophil infiltration and TNF-α production in the lungs of mice challenged with lethal influenza virus infection (12).

CONCLUSION

These studies demonstrated that AAAG ODN could alleviate the system inflammatory responses induced by burn injury, and the effect was correlated with

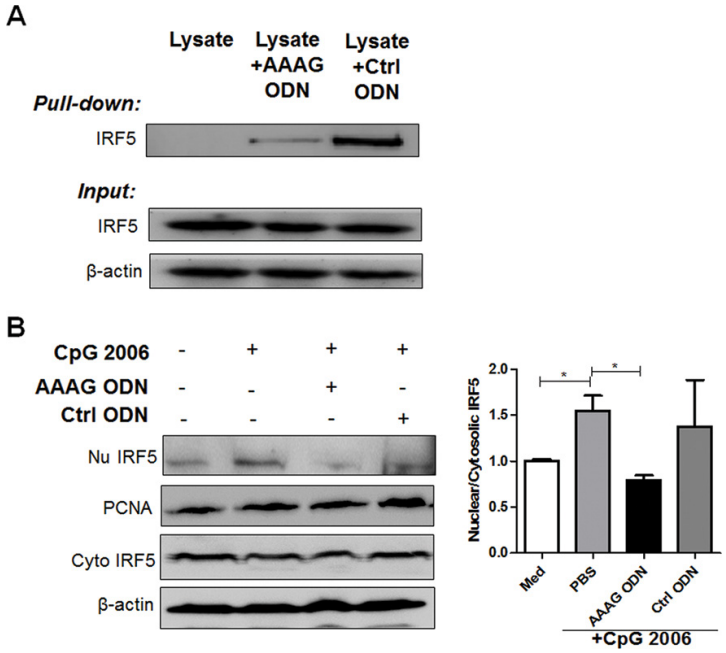

Figure 6. The interfering role of AAAG ODN on IRF5. (A) Binding of AAAG ODN with IRF5. The proteins in IRF5 expressing HEK293 cells were pulled down using AAAG ODN or control ODN-coated beads, and analyzed by Western blot with IRF5 monoclonal antibodies. (B) Inhibition of AAAG ODN on nuclear translocation of IRF5. The THP-1 cells were incubated with CpG 2006 plus AAAG ODN or control ODN for 24 h, then harvested to separate cytoplasmic and nuclear fractions. The proteins in each fraction were recognized by IRF5 antibodies by Western blot. Nu IRF5: IRF5 in nucleus; Cyto IRF5: IRF5 in cytoplasm. The data are from three independent experiments and are represented as mean ± SEM. $^{*}P < 0.05$, $^{**}P < 0.01$, $^{***}P < 0.001$.

AAAG ODN–mediated inhibition of nuclear translocation of IRF5. The data suggested that AAAG ODN could act as a cytoplasmic decoy capable of interfering the function of IRF5 and be developed as a drug candidate for the treatment of inflammatory diseases.

Together, the data presented here may provide an experimental basis for understanding how IRF5 is involved in overwhelming acute systemic inflammation, and for developing AAAG ODN as a medication candidate for the treatment of SIRS caused by sterile damage such as severe burn injury or pathogen infection via interfering IRF5.

ACKNOWLEDGMENTS

The authors would like to thank Leichao Zhang, Jiwei Liu and Xian Zhang for technical assistance, and acknowledge the contribution of Wei Sun, Xiuping Meng and Shu Nie for analysis strategies. This work was supported by the National Nature Scientific Foundation of China (81471888, 81570002 and 31670937).

DISCLOSURE

The authors declare that they have no competing interests as defined by *Molecular Medicine*, or other interests that might be perceived to influence the results and discussion reported in this paper.

REFERENCES

1. Zhang Q, *et al.* (2010) Circulating mitochondrial DAMPs cause inflammatory responses to injury. *Nature.* 464:104–7.
2. Manson J, Thiemermann C, Brohi K. (2012) Trauma alarmins as activators of damage-induced inflammation. *Br. J. Surg.* 99 Suppl 1:12–20.
3. Kandimalla ER, Zhu FG, Bhagat L, Yu D, Agrawal S. (2003) Toll-like receptor 9: modulation of recognition and cytokine induction by novel synthetic CpG DNAs. *Biochem. Soc. Trans.* 31:654–8.
4. Takaoka A, *et al.* (2005) Integral role of IRF-5 in the gene induction programme activated by Toll-like receptors. *Nature.* 434:243–9.
5. Chen W, *et al.* (2008) Insights into interferon regulatory factor activation from the crystal structure of dimeric IRF5. *Nat. Struc. Mol. Biol.* 15:1213–20.
6. Pelka K, Latz E. (2013) IRF5, IRF8, and IRF7 in human pDCs: the good, the bad, and the insignificant? *Eur. J. Immunol.* 43:1693–7.
7. Steinhagen F, *et al.* (2013) IRF-5 and NF-kappaB p50 co-regulate IFN-beta and IL-6 expression in TLR9-stimulated human plasmacytoid dendritic cells. *Eur. J. Immunol.* 43:1896–906.
8. Sandling JK, *et al.* (2010) A candidate gene study of the type I interferon pathway implicates IKBKE and IL8 as risk loci for SLE. *Eur. J. Hum. Genet.* 19:479–84.
9. Allen TC, Kurdowska A. (2014) Interleukin 8 and Acute Lung Injury. *Arch. Pathol. Lab. Med.* 138:266–9.
10. Ren JY, Chen X, J.C ZJ. (2014) IKKβ is an IRF5 kinase that instigates inflammation. *PNAS.* 111:17438–43.
11. Weiss M, *et al.* (2015) IRF5 controls both acute and chronic inflammation. *Proc. Natl. Acad. Sci. USA.* 112:11001–6.
12. Fang M, *et al.* (2011) An oligodeoxynucleotide capable of lessening acute lung inflammatory injury in mice infected by influenza virus. *Biochem. Biophys. Res. Commun.* 415:342–7.
13. Wei Z, *et al.* (2016) Mangiferin inhibits macrophage classical activation via downregulating interferon regulatory factor 5 expression. *Mol. Med. Rep.* 14:1091–8.
14. Zhu W, *et al.* (2016) Baicalin ameliorates experimental inflammatory bowel disease through polarization of macrophages to an M2 phenotype. *Int. Immunopharmacol.* 35:119–26.
15. Li J, Liu Y, Xu H, Fu Q. (2016) Nanoparticle-Delivered IRF5 siRNA Facilitates M1 to M2 Transition, Reduces Demyelination and Neurofilament Loss, and Promotes Functional Recovery After Spinal Cord Injury in Mice. *Inflammation.* 39:1704–17.
16. Committee for the Update of the Guide for the Care and Use of Laboratory Animals, Institute for Laboratory Animal Research, Division on Earth and Life Studies. (2011) *Guide for the Care and Use of Laboratory Animals*, 8th ed.
17. Zins SR, Amare MF, Anam K, Elster EA, Davis TA. (2010) Wound trauma mediated inflammatory signaling attenuates a tissue regenerative response in MRL/MpJ mice. *J. Inflamm. Res.* 7:25.
18. McGill MR, *et al.* (2014) Serum mitochondrial biomarkers and damage-associated molecular patterns are higher in acetaminophen overdose patients with poor outcome. *Hepatology.* 60:1336–45.
19. Dancey DR, *et al.* (1999) ARDS in patients with thermal injury. *Intensive Care Med.* 25:1231–6.

20. Ipaktchi K, *et al.* (2006) Attenuating burn wound inflammatory signaling reduces systemic inflammation and acute lung injury. *J. Immunol.* 177:8065–71.
21. Schwacha MG, Holland LT, Chaudry IH, Messina JL. (2005) Genetic variability in the immune-inflammatory response after major burn injury. *Shock.* 23:123–8.
22. Davis TA, et al. (2009) Extracorporeal shock wave therapy suppresses the early proinflammatory immune response to a severe cutaneous burn injury. *Int. Wound J.* 6:11–21.
23. Zhang J, Sio SW, Moochhala S, Bhatia M. (2010) Role of hydrogen sulfide in severe burn injury-induced inflammation in mice. *Mol. Med.* 16:417–24.
24. Costantini TW, et al. (2009) Burns, inflammation, and intestinal injury: protective effects of an anti-inflammatory resuscitation strategy. *J. Trauma.* 67:1162–8.
25. Nakazawa H, et al. (2017) iNOS as a Driver of Inflammation and Apoptosis in Mouse Skeletal Muscle after Burn Injury: Possible Involvement of Sirt1 S-Nitrosylation-Mediated Acetylation of p65 NF-kappaB and p53. *PloS One.* 12:e0170391.
26. Csontos C, et al. (2010) Time course of pro- and anti-inflammatory cytokine levels in patients with burns: prognostic value of interleukin-10. *Burns*. 36:483–94.
27. Jeschke MG, et al. (2011) Insulin protects against hepatic damage postburn. *Mol. Med*. 17:516–22.
28. Baird A, et al. (2016) Mice engrafted with human hematopoietic stem cells support a human myeloid cell inflammatory response in vivo. *Wound Repair Regen.* 24:1004–14.
29. Takao K, Miyakawa T. (2015) Genomic responses in mouse models greatly mimic human inflammatory diseases. *Proc. Natl. Acad. Sci. USA.* 112:1167–72.
30. Chen Z, Zhang Y, Ma L, Ni Y, Zhao H. (2016) Nrf2 plays a pivotal role in protection against burn trauma-induced intestinal injury and death. *Oncotarget*. 7:19272–83.
31. Kerby JD, et al. (2006) Sex differences in mortality after burn injury: results of analysis of the National Burn Repository of the American Burn Association. *J. Burn Care Res.* 27:452–6.
32. Faggioni R, Moser A, Feingold KR, Grunfeld C. (2000) Reduced leptin levels in starvation increase susceptibility to endotoxic shock. *Am. J. Pathol.* 156:1781–7.
33. Okorokov PL, et al. (2012) [Nutritional factors of inflammation induction or lipid mechanism of intestinal endotoxin transport]. *Fiziologiia Cheloveka.* 38:105–12.
34. Dahiya P. (2009) Burns as a model of SIRS. *Front. Biosci. (Landmark Ed.)* 14:4962–7.
35. Nishiura T, et al. (2000) Gene expression and cytokine and enzyme activation in the liver after a burn injury. *J. Burn Care Rehabil.* 21:135–41.
36. Yamamoto M, Sato T, Beren J, Verthelyi D, Klinman DM. (2011) The acceleration of wound healing in primates by the local administration of immunostimulatory CpG oligonucleotides. *Biomaterials.* 32:4238–42.
37. Farina A, et al. (2014) Epstein-Barr virus infection induces aberrant TLR activation pathway and fibroblast-myofibroblast conversion in scleroderma. *J. Invest. Dermatol.* 134:954–64.
38. Paun A, et al. (2008) Functional characterization of murine interferon regulatory factor 5 (IRF-5) and its role in the innate antiviral response. *J. Biol. Chem.* 283:14295–308.
39. Speranskii AI, Kostyuk SV, Kalashnikova EA, Veiko NN. (2016) [Enrichment of extracellular DNA from the cultivation medium of human peripheral blood mononuclears with genomic CpG rich fragments results in increased cell production of IL-6 and TNF-a via activation of the NF-kB signaling pathway]. *Biomeditsinskaia Khimiia.* 62:331–40.
40. Barnes BJ, Kellum MJ, Field AE, Pitha PM. (2002) Multiple Regulatory Domains of IRF-5 Control Activation, Cellular Localization, and Induction of Chemokines that Mediate Recruitment of T Lymphocytes. *Mol. Cell. Biol.* 22:5721–40.
41. Ikushima H, Negishi H, Taniguchi T. (2013) The IRF family transcription factors at the interface of innate and adaptive immune responses. *Cold Spring Harb. Symp. Quant. Biol.* 78:105–16.
42. Xu H, *et al.* (2012) 4F decreases IRF5 expression and activation in hearts of tight skin mice. *PloS One.* 7:e52046.
43. Garg T, Rath G, Goyal AK. (2015) Comprehensive review on additives of topical dosage forms for drug delivery. *Drug Delivery*. 22:969–87.
44. Glavas-Dodov M, et al. (2003) 5-fluorouracil in topical liposome gels for anticancer treatment: formulation and evaluation. *Acta Pharmaceutica*. 53:241–50.
45. Lomas-Neira J, Perl M, Venet F, Chung CS, Ayala A. (2012) The role and source of tumor necrosis factor-alpha in hemorrhage-induced priming for septic lung injury. *Shock.* 37:611–20.
46. Zheng H, *et al.* (2005) Ligustrazine attenuates acute lung injury after burn trauma. *Burns.* 31:453–8.
47. Osuchowski MF, Welch K, Siddiqui J, Remick DG. (2006) Circulating cytokine/inhibitor profiles reshape the understanding of the SIRS/CARS continuum in sepsis and predict mortality. *J. Immunol.* 177:1967–74.

Cite this article as: *Xiao* Y, *et al.* (2017) An oligodeoxynucleotide with AAAG repeats significantly attenuates burn-induced systemic inflammatory responses by inhibiting interferon regulatory factor 5 pathway. *Mol. Med*. 23:166–76.